

# An Efficient and Accessible Hectogram-Scale Synthesis for the Selective O-GlcNAcase Inhibitor Thiamet-G

Viktor Holicek, Matthew Deen, Sandeep Bhosale, Roger A. Ashmus, and David J. Vocadlo\*

Cite This: *ACS Omega* 2024, 9, 49223–49228

Read Online

ACCESS |



Metrics &amp; More

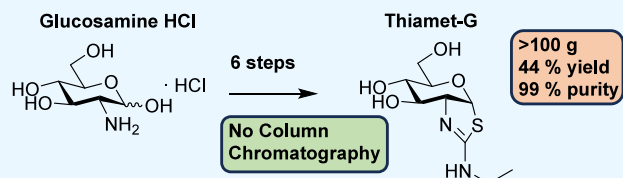


Article Recommendations



Supporting Information

**ABSTRACT:** Altered levels of intracellular protein glycosylation with O-linked  $\beta$ -N-acetylglucosamine (O-GlcNAc) have emerged as being involved in various cancers and neurodegenerative diseases. OGA inhibitors have proven critically useful as tools to help understand the roles of O-GlcNAc, yet accessing large quantities of inhibitors necessary for many animal studies remains a challenge. Herein is described a scalable method to produce Thiamet-G, a potent, selective, and widely used brain-permeable OGA inhibitor. This synthetic route begins with inexpensive precursor, requires no column chromatography, employs simple nontoxic reagents, and in a single campaign can furnish several hundred grams of crystalline Thiamet-G in an overall yield of 44% over six steps.



## INTRODUCTION

The O-linked glycosylation of hydroxyl groups of serine and threonine residues of nuclear and cytoplasmic proteins with N-acetylglucosamine (O-GlcNAc) is a post-translational modification (PTM) found on well over a thousand proteins.<sup>1,2</sup> O-GlcNAc has been proposed to play roles in numerous cellular processes and is implicated in various diseases including, most notably, cancers<sup>3–6</sup> and neurodegenerative diseases, including both Alzheimer's Disease (AD)<sup>7,8</sup> and Parkinson's Disease (PD).<sup>9–11</sup> However, the molecular basis by which altered O-GlcNAc levels influence cellular pathways and the pathophysiology of cancers and human neurodegenerative diseases are ill-defined and remain topics of high interest.

Interestingly, there are only two enzymes that control this dynamic post-translational modification. O-GlcNAc is installed by O-GlcNAc transferase (OGT) and removed by O-GlcNAcase (OGA), a family 84 glycosidase hydrolase (GH84).<sup>12</sup> One important and widely used class of chemical tools for studying this relationship are potent and selective inhibitors of OGA, which can be used to increase levels of cellular O-GlcNAcylation in different model systems. Accordingly, both academic and industrial teams have worked to develop potent and selective OGA inhibitors to study the physiological function of OGA in animal models of neurodegeneration toward the development of potential therapeutics.

While several OGA inhibitors have been reported, including some from industry derived high-throughput screening medicinal chemistry optimization campaigns (Figure 1) such as MK-8719,<sup>13</sup> ASN90,<sup>14</sup> and LY3372689,<sup>15</sup> the compound that has seen the widest use is Thiamet-G.

The design of Thiamet-G was inspired by mechanistic studies of the OGA enzyme showing the enzyme uses a two-step reaction involving an oxazoline intermediate.<sup>16</sup> These

mechanistic insights led to the preparation of the transition state analog Thiamet-G, which is one of the most potent ( $K_i = 2.1$  nM) and selective (37,000 fold selectivity hOGA over  $\beta$ -hexosaminidase<sup>17</sup>) compounds currently reported. Genetic deficiencies in  $\beta$ -hexosaminidase resulting in its inability to cleave glycoconjugates from gangliosides are responsible for the manifestation of the orphan congenital diseases known as Tay Sachs and Sandhoff's. The importance of hOGA selectivity was highlighted by the problematic off-target effects observed in the first reported inhibitors that inadvertently also targeted  $\beta$ -hexosaminidase.<sup>18</sup> As an hOGA inhibitor, Thiamet-G is orally bioavailable, permeates into the brain, and has accordingly been used to study in vivo O-GlcNAcylation and its role in the pathology of inflammation,<sup>19</sup> cardiovascular disease,<sup>20,21</sup> cancers,<sup>4,6</sup> stroke,<sup>22</sup> AD,<sup>7,9,23</sup> PD,<sup>16,24</sup> Progressive Supranuclear Palsy (PSP),<sup>25</sup> and Huntington's Disease (HD).<sup>26</sup> However, due to the modest permeability of Thiamet-G, coupled with extended dosing needed in transgenic animal studies of neurodegenerative diseases, these studies often require large quantities of Thiamet-G for chronic long-term dosing administered via drinking water (>100 mg  $\text{kg}^{-1} \text{ day}^{-1}$ ).<sup>9,16,23,25,27–29</sup> The requirement for large amounts of material limits the feasibility of these studies within academic settings. Unfortunately, the current synthetic route for Thiamet-G is unsuitable for preparing large quantities in academic laboratories due to its reliance on toxic heavy metals

Received: July 2, 2024

Revised: October 18, 2024

Accepted: October 28, 2024

Published: December 8, 2024



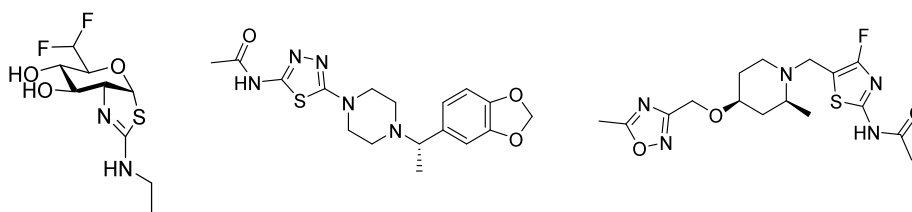


Figure 1. Competitive OGA inhibitors MK-8719 (left), ASN90 (center), and LY3372689 (right).

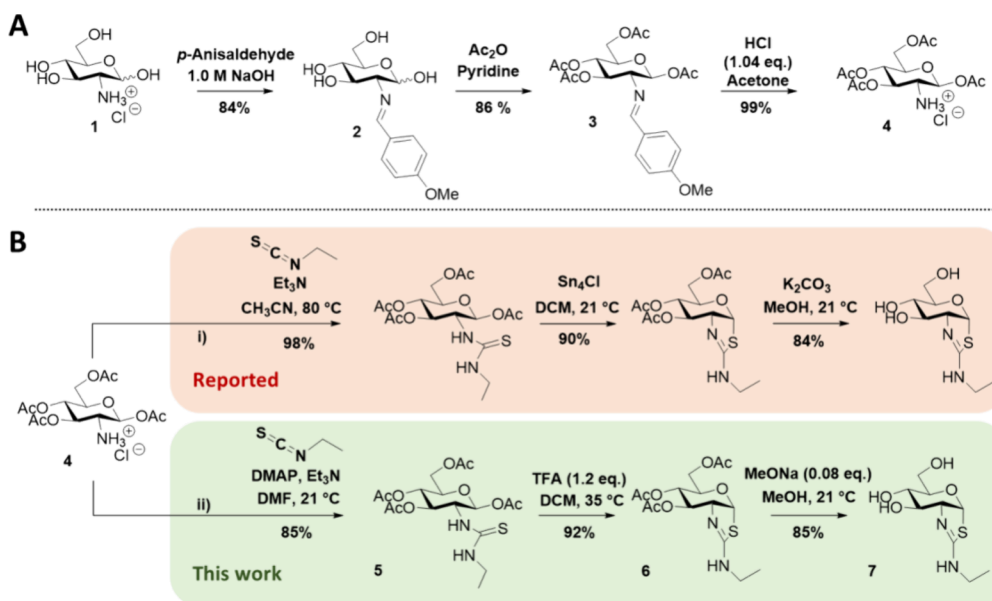
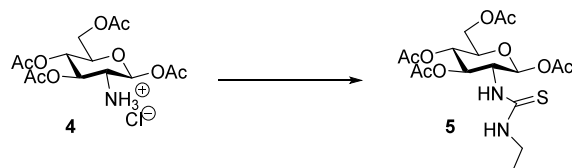


Figure 2. Synthetic routes to Thiamet-G. Upper pathway (A) Synthetic route used to access central intermediate 4 (yields given for large-scale reactions). (B) Comparison of the new and previously reported synthetic routes to Thiamet-G.

Table 1. Optimization of Conditions for the Formation of the Thiourea Intermediate 3<sup>4a</sup>



condition	catalyst	cat. equiv	EIT equiv	solvent	temp. (°C)	solvent (M)	time (h)	yield (%)
reported <sup>16</sup>			3.0	MeCN	80	0.06		96
1			3.0	DCM	25	0.1	96	49
2			3.0	pyridine	25	0.1	48	88
3			3.0	MeCN	25	0.1	72	65
4	pyridine	0.20	1.2	MeCN	25	0.1	48	74
5	DMAP	0.20	1.2	ACN	25	0.1	48	71
6	DMAP	0.02	1.2	MeCN	50	0.1	24	42
7	pyridine	0.20	1.2	DMF	25	0.1	24	78
8	DMAP	0.02	1.2	DMF	25	0.1	36	76
9	DMAP	0.02	1.2	DMF	25	1.0	36	85

<sup>4a</sup>The listed reactions were carried out on a 1.0 gram scale quantity in the presence of 1.8 equiv of triethylamine unless otherwise noted.

and column chromatography.<sup>16</sup> Furthermore, MK-8719 and many analogs of Thiamet-G use this compound as an advanced intermediate, making improved routes to Thiamet-G of value. Thiamet-G has also found use in inhibitor cross-competition enzyme kinetics studies to orthogonally validate the binding site for other OGA targeting molecules, including ASN90.<sup>14</sup> As such, there is a need for a more accessible and straightforward synthetic route to Thiamet-G to support this field of research.

## RESULTS AND DISCUSSION

In looking to develop a scalable synthesis, the previously reported synthetic method (Figure 2) was adapted. This route goes through the well-characterized intermediate, 1,3,4,6-tetra-*O*-acetyl-2-amino-2-deoxy- $\beta$ -D-glucopyranose hydrochloride (4), the gram-scale synthesis of which is well established (Figure 2A).<sup>30</sup> Starting from the inexpensive and readily available glucosamine hydrochloride salt (1) was isolated

kilogram quantities of **4** in three steps (66% yield compared to the 43% reported yield)<sup>30</sup> using materials and reaction vessels available within an academic setting. Furthermore, through modification of washing and extraction volumes, the solvent waste stream was reduced by over 25%.

With compound **4** in hand, the next aim was to scale up the installation and subsequent cyclization of the C-2 ethyl thiourea group. Employing the previously published conditions (Figure 2B) of triethylamine and ethyl isothiocyanate refluxed in acetonitrile failed to reproduce the reported 98% yield<sup>16</sup> of thiourea containing compound **5**. Moreover, incomplete conversion of the starting material was observed, which necessitated flash silica column chromatography to isolate product. Looking to improve the reliability of this reaction and circumvent the need for heating, pyridine was substituted as a solvent, which resulted in the reaction being completed within 48 h at room temperature. It was reasoned that pyridine might be functioning as a nucleophilic catalyst and facilitating complete conversion of the amine starting material. This in turn led to examining the use of substoichiometric quantities of pyridine as an additive in the original reaction conditions (Table 1, condition 4). These new conditions decreased the amount of time to completion of the reaction while also eliminating the need for heating the reaction to reflux. To further minimize the volume of pyridine needed, 4-dimethylaminopyridine (DMAP) as a catalyst in place of pyridine was examined. Optimizing the fractional equivalencies of either DMAP or pyridine as nucleophilic catalysts in acetonitrile allowed the reaction to proceed efficiently at room temperature while also enabling the use of reduced equivalents of ethyl isothiocyanate. Further, switching the reaction solvent from acetonitrile to dimethylformamide (DMF) reduced the required reaction times and enabled reducing the catalyst to 0.02 equiv (entry 8). Finally, the increased solubility of the starting materials and product in DMF enabled increasing the reaction concentration by 10-fold to 1.0 M. Accordingly, it was feasible to run the reaction at 400 g (1 mol) scale within a standard 3 L round-bottom flask without the need for reflux condensation or column chromatography.

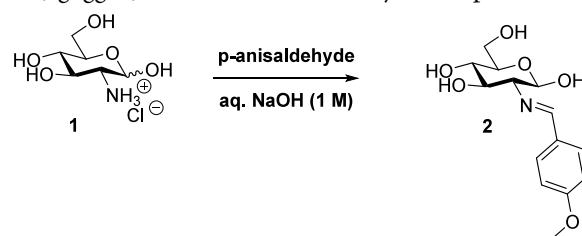
Following the installation of the thiourea, methods to manipulate intramolecular cyclization to obtain thiazoline **6** in a scalable manner were explored. Previously published methods carried out this transformation using 4 equiv of tin(IV) chloride as a Lewis acid catalyst.<sup>31</sup> To avoid the use of multihundred-gram quantities of this toxic reagent, various Brønsted acids were examined as alternatives. Trifluoroacetic acid has previously been shown as an effective cyclization reagent for the synthesis of thiazolines at room temperature.<sup>32</sup> Using just 1.2 equiv of trifluoroacetic acid at room temperature, efficient cyclization of compound **5** was observed, with the resulting crude compound **6** being of sufficient purity to move forward into subsequent reactions. To enable the use of standard academic setting glassware, the concentration of the limiting reactant was increased from 0.1 to 0.25 M with no resultant impact on either yield or product purity. At the suggestion of the reviewers and considering changing regulations and industry practices demanding a shift away from chlorinated solvents like dichloromethane (DCM), additional solvent substitutes were retroactively explored for this step. Using thin-layer chromatography and mass spectrometry to monitor reaction conversion progress, it was observed that acetonitrile and ethyl acetate were able to achieve >99% consumption of the starting material (**5**) and

conversion to yield the thiazoline (**6**) within the same time frame, the same temperature, and the same concentration of reactants as used in the DCM based protocol. Additional solvents tested in identical conditions including 1,4-dioxane, THF, 2-MeTHF, DMF, and NMP all failed to fully consume the starting material within 24 h. The authors suspect that acetonitrile and ethyl acetate would perform equally well at larger scales, and thus believe both solvents to be superior to DCM as less toxic and less environmentally harmful substitutes.

De-O-acetylation of **6** to yield the final product Thiamet-G (**7**) was completed using catalytic amounts of sodium methoxide (0.05 equiv) in anhydrous methanol. While it is common to neutralize the base in such Zemplén reactions using acidic resin, the reaction workup was simplified by applying a quantity of sodium bisulfate equimolar to that of the base. The resulting insoluble sodium sulfate solid was conveniently removed via filtration through a pad of Celite. In this way, it was possible to isolate pure Thiamet-G by crystallization from a mixture of methanol and ethyl acetate. This route (Figure 2B) delivered the desired Thiamet-G in high purity with an overall yield of 66% over three steps from **4** and 44% yield across six steps beginning from the readily available hydrochloride salt **1** with no column purifications.

## EXPERIMENTAL SECTION

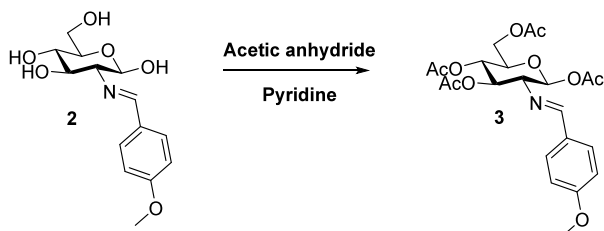
Thin-layer chromatography (TLC) was performed using Merck silica gel 60 F254 aluminum-backed plates that were stained by heating ( $\geq 200$  °C) with 5% sulfuric acid in ethanol or with a solution of phosphomolybdic acid (2.5% w/v), cerium sulfate (1% w/v), and sulfuric acid (6% v/v) in water. High pressure liquid chromatography (HPLC) was performed on an Agilent 1100 series device equipped with a variable wavelength UV–vis detector using ZORBAX 300SB C8 column (5.0  $\mu\text{m}$ , 9.4  $\times$  250 mm for analytical runs and semipreparative scale purifications) and elution carried out using HPLC grade solvents. To concentrate reaction mixtures solvents were evaporated under reduced pressure on a rotary evaporator between 40 and 60 °C using either a PIAB vacuum system or Welch W Series high vacuum oil pump. NMR spectra were recorded on Bruker AVANCE III 400 or AVANCE II 600 QNP. Spectra are referenced according to the chemical shift of the deuterated solvent in which they were dissolved (<sup>1</sup>H NMR: CDCl<sub>3</sub>: 7.26 ppm, CD<sub>3</sub>OD: 3.30 ppm; <sup>13</sup>C{<sup>1</sup>H} NMR: CDCl<sub>3</sub>: 77.0 ppm; CD<sub>3</sub>OD 49.0 ppm) and peak assignments were made on the basis of 2D-NMR (<sup>1</sup>H COSY, HSQC, HMBC) experiments. High resolution mass spectra (HRMS) were recorded on a Bruker MaXis Impact spectrometers using positive or negative electrospray ionization (ESI). All reactions were carried out within the confines of an ISO 9001:2000 compliant fume hood with operators wearing full PPE including lab coats, chemical resistant butyl rubber gloves, goggles, and 75SCP100L Honeywell respirators.



**2-Deoxy-2-[[4-methoxyphenyl)methylene]amino]- $\beta$ -D-glucopyranose (2).** Using a 20 L polypropylene bucket sitting in a 83 L polyethylene Rubbermaid 0 °C ice bath secondary container, a solution of glucosamine hydrochloride (2.044 kg, 9.48 mol) in NaOH (1 M, 9.48 L) was prepared to which p-anisaldehyde (1.15 L, 9.48 mol) was added dropwise over 30 min under mechanical stirring. The resulting mixture was stirred at 0 °C for 1 h and the precipitate was collected by a 4 L Buchner funnel suction filtration, washed successively with cold water (9.5 L), cold ethanol (9.5 L) and diethyl ether (9.5 L), and then dried under vacuum to give the title compound as a white solid. (2.37 kg, 84% yield).

$^1\text{H}$  NMR (400 MHz, Methanol- $d_4$ )  $\delta$  8.13 (s, 1H), 7.76–7.66 (m, 2H), 7.03–6.92 (m, 2H), 6.53 (d,  $J$  = 6.8 Hz, 1H), 4.94 (d,  $J$  = 5.2 Hz, 1H), 4.83 (d,  $J$  = 5.5 Hz, 1H), 4.75–4.66 (m, 1H), 4.56 (t,  $J$  = 5.8 Hz, 1H), 3.80 (s, 3H), 3.73 (ddd,  $J$  = 11.7, 5.7, 2.0 Hz, 1H), 3.50 (dt,  $J$  = 13.0, 6.6 Hz, 1H), 3.43 (dt,  $J$  = 9.0, 4.4 Hz, 1H), 3.24 (ddd,  $J$  = 9.8, 5.8, 2.1 Hz, 1H), 3.19–3.11 (m, 1H), 2.80 (dd,  $J$  = 9.3, 7.7 Hz, 1H).

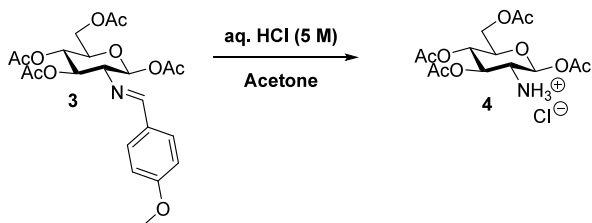
$^{13}\text{C}\{^1\text{H}\}$  NMR (101 MHz, DMSO)  $\delta$  191.7, 164.7, 161.7, 161.5, 132.3, 130.2, 130.1, 129.6, 115.0, 114.4, 96.1, 78.7, 77.3, 75.1, 70.9, 61.8, 56.2, 55.7.



**1,3,4,6-Tetra-O-acetyl-2-deoxy-2-[[4-methoxyphenyl)methylene]amino]- $\beta$ -D-glucopyranose (3).** In a 20 L polypropylene bucket housed in an 83 L polyethylene 0 °C ice bath secondary container Imine (2) (700 g, 2.35 mol) and pyridine (3.0 L, 37.6 mol) were stirred for 5 min 0 °C. Acetic anhydride (5.52 L, 58.4 mol) was then added slowly over the course of 2 h with continuous stirring. The reaction mixture was maintained at 0 °C for 2 h and then at room temperature overnight. The reaction was quenched transferring 1.0 L portions of the reaction into 4.0 L of ice water at 0 °C. The precipitate was collected by 4 L Buchner funnel suction filtration, washed with 4.0 L of ice water and dried under vacuum to give the title compound as a white solid (943 g, 86% yield).

$^1\text{H}$  NMR (400 MHz, Chloroform- $d$ )  $\delta$  8.18 (s, 1H), 7.74–7.63 (m, 2H), 6.96–6.91 (m, 2H), 5.96 (d,  $J$  = 8.3 Hz, 1H), 5.45 (t,  $J$  = 9.6 Hz, 1H), 5.16 (dd,  $J$  = 10.1, 9.5 Hz, 1H), 4.40 (dd,  $J$  = 12.4, 4.6 Hz, 1H), 4.15 (dd,  $J$  = 12.4, 2.1 Hz, 1H), 3.99 (ddd,  $J$  = 10.1, 4.6, 2.2 Hz, 1H), 3.86 (s, 3H), 3.47 (dd,  $J$  = 9.8, 8.3 Hz, 1H), 2.12 (s, 3H), 2.06 (s, 3H), 2.04 (s, 3H), 1.90 (s, 3H).

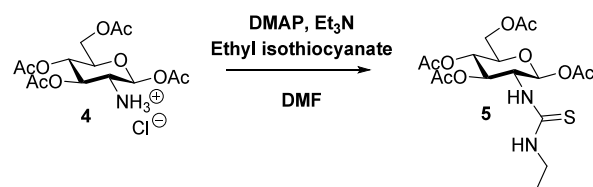
$^{13}\text{C}\{^1\text{H}\}$  NMR (101 MHz, Chloroform- $d$ )  $\delta$  170.7, 169.9, 169.5, 168.8, 164.3, 162.3, 130.3, 128.3, 114.1, 93.2, 77.2, 73.3, 73.0, 72.8, 68.1, 61.9, 55.4, 20.8, 20.8, 20.7, 20.5.



**1,3,4,6-Tetra-O-acetyl-2-amino-2-deoxy- $\beta$ -D-glucopyranose (4).** In a 20 L polypropylene bucket housed in an 83 L polyethylene secondary container, a solution of acetoxy imine (1.09 kg, 2.34 mol) in acetone (7.8 L) was treated with 5 M HCl (486 mL, 2.43 mol). The solution was stirred for 30 min before diethyl ether (3.6 L) was added, and the stirring was continued for a further 1 h. The precipitate was collected via 4 L Buchner funnel suction filtration, washed twice with 4.0 L of cold diethyl ether and dried under vacuum to give the title compound as a white solid (885 g, 99% yield).

$^1\text{H}$  NMR (400 MHz, DMSO- $d_6$ )  $\delta$  6.05–5.80 (m, 1H), 5.35 (ddt,  $J$  = 10.6, 9.1, 2.8 Hz, 1H), 4.92 (dd,  $J$  = 10.2, 9.2 Hz, 1H), 4.18 (dd,  $J$  = 12.4, 4.3 Hz, 1H), 4.01 (ddd,  $J$  = 22.2, 10.1, 3.7 Hz, 2H), 3.65–3.45 (m, 1H), 2.16 (s, 3H), 2.02 (s, 3H), 1.99 (s, 3H), 1.96 (s, 3H).

$^{13}\text{C}\{^1\text{H}\}$  NMR (101 MHz, DMSO- $d_6$ )  $\delta$  170.4, 170.2, 169.8, 169.1, 90.6, 72.1, 70.8, 68.3, 61.7, 52.6, 21.4, 21.3, 21.0, 20.8.

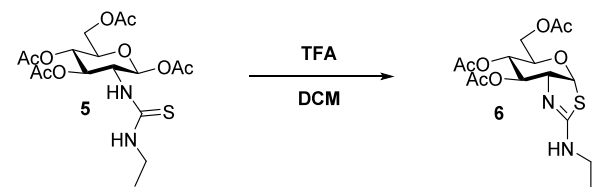


**1,3,4,6-Tetra-O-acetyl-2-deoxy-2-ethylthioureido- $\beta$ -D-glucopyranose (5).** In a 3.0 L round-bottom flask 1,3,4,6-tetra-acetyl glucosamine hydrochloride (400 g, 1.04 mol) and DMAP (2.55 g, 0.02 mmol) were suspended in anhydrous DMF (1.0 L). Triethylamine (256 mL, 1.84 mol) was added to the suspension in a dropwise fashion over 30 min, after which the suspension fully dissolved. Ethyl isothiocyanate (110 mL, 1.25 mol) was added to the reaction mixture over 2.5 h using a dropping funnel. The reaction was then stirred at room temperature for 48 h. Following reaction completion as judged by TLC (95%  $\text{CH}_2\text{Cl}_2$ , 5% MeOH v/v) the mixture was diluted with 4 L of DCM and washed sequentially with a 4 L solution water and brine (50% v/v), 4L of 0.01 M HCl, 4 L of saturated  $\text{NaHCO}_3$ , and 4 L of brine. The organic layer was then dried using sodium sulfate and concentrated with a toluene azeotrope yielding the product as a dark yellow viscous liquid (384 g, 85% yield).

$^1\text{H}$  NMR (400 MHz,  $\text{CDCl}_3$ )  $\delta$  6.14 (t,  $J$  = 5.2 Hz, 1H), 5.98 (s, 1H), 5.75 (d,  $J$  = 8.5 Hz, 1H), 5.28–5.15 (m, 2H), 4.30 (dd,  $J$  = 12.5, 4.6 Hz, 1H), 4.16 (dd,  $J$  = 12.5, 2.3 Hz, 1H), 3.85 (ddt,  $J$  = 6.3, 4.4, 2.2 Hz, 1H), 3.43 (s, 2H), 2.16 (s, 3H), 2.12 (s, 3H), 2.09 (s, 3H), 2.07 (s, 3H), 1.22 (t,  $J$  = 7.2 Hz, 3H).

$^{13}\text{C}\{^1\text{H}\}$  NMR (151 MHz,  $\text{CDCl}_3$ )  $\delta$  171.7, 170.8 169.8, 169.6, 169.3, 93.0, 73.0, 72.8, 67.7, 63.1, 61.7, 21.1, 20.9, 20.8, 20.6, 14.8, 14.1.

HR-ESI-MS calculated for  $\text{C}_{17}\text{H}_{26}\text{N}_2\text{O}_9\text{S}$   $[\text{M} + \text{H}]^+$  435.1359, found 435.1431



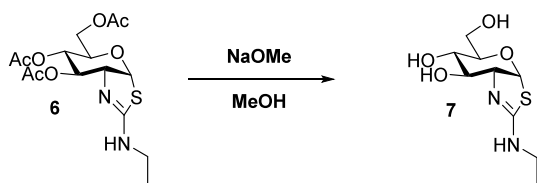
**3,4,6-Tri-O-acetyl-1,2-dideoxy-2'-ethylamino- $\alpha$ -D-glucopyranoso-[2,1- $d$ ]- $\Delta^2$ '-thiazoline (6).** Compound 5 (350 g, 0.805 mol) was dissolved in DCM (3.3 L). After addition of

TFA (74 mL, 0.969 mol) the reaction mixture was then heated to reflux with a heating mantle for 24 h and the reaction was completed as judged by TLC (95% CH<sub>2</sub>Cl<sub>2</sub> 5% MeOH v/v). The resulting crude mixture was filtered through a pad of Celite and washed with saturated NaHCO<sub>3</sub>. The resulting organic layer was concentrated in-vacuo to give the cyclized product as a flaky light yellow solid (278 g, 92% yield).

<sup>1</sup>H NMR (400 MHz, CDCl<sub>3</sub>) δ 6.23 (d, *J* = 6.5 Hz, 1H), 5.43 (dd, *J* = 4.1, 2.7 Hz, 1H), 4.95 (ddd, *J* = 9.5, 2.7, 1.1 Hz, 1H), 4.36 (ddd, *J* = 6.5, 4.1, 1.1 Hz, 1H), 4.21–4.09 (m, 2H), 3.90–3.79 (m, 1H), 3.46–3.20 (m, 2H), 2.11 (s, 3H), 2.08 (s, 3H), 2.07 (s, 3H), 1.21 (t, *J* = 7.2 Hz, 3H).

<sup>13</sup>C{<sup>1</sup>H} NMR (151 MHz, CDCl<sub>3</sub>) δ 170.7, 169.7, 169.5, 89.6, 72.7, 71.9, 69.1, 68.5, 63.2, 39.5, 21.1, 20.9, 20.8, 14.9, 1.04.

HR-ESI-MS calculated for C<sub>15</sub>H<sub>22</sub>N<sub>2</sub>O<sub>7</sub>S [M + H]<sup>+</sup> 375.1148, found 375.1258.



**1,2-Dideoxy-2'-ethylamino- $\alpha$ -D-glucopyranoside-[2,1- $\delta$ ]- $\Delta$ 2'-thiazoline (7).** Compound 6 (278 g, 0.74 mol) was dissolved into 2.97 L of anhydrous methanol (0.25 M solution) followed by addition of 0.2 M sodium methoxide (185 mL, 37.1 mmol). The mixture was then stirred at room temperature until the reaction was judged to be complete by TLC (95% CH<sub>2</sub>Cl<sub>2</sub> 5% MeOH v/v). The reaction was quenched using a 1.0 M aqueous solution of equimolar sodium bisulfate (37.1 mL, 37.1 mmol) and subsequently filtered through a pad of Celite before concentrating the resulting organic layer in-vacuo. The product was isolated via recrystallization of the crude dried material in 9:1 MeOH EtOAc to yield crude Thiamet-G.

**Recrystallization of Thiamet-G (7).** Crude Thiamet-G was completely dissolved in a minimal volume of 9:1 MeOH EtOAc (10 mL/g) with the aid of heating (55 °C) and rotational mixing via the rotary evaporator and bath under atmospheric pressure. Once dissolved, the solution was allowed to cool to room temperature and then placed in a –20 °C freezer overnight. The next day, the precipitate was collected via Buchner funnel vacuum filtration and rinsed with chilled 9:1 MeOH EtOAc. The resulting supernatant was used for further recrystallization. After three cycles of recrystallization, the consolidated Thiamet-G was isolated as an off white amorphous solid (157 g, 85% yield, 99.6% pure).

Decomposition point 143 °C.

Elemental analysis, Predicted: C 43.54% H 6.50% N 11.28%, Found: C 43.70% H 6.36% N 11.25%.

<sup>1</sup>H NMR (600 MHz, Methanol-*d*<sub>4</sub>) δ 6.29 (d, *J* = 6.3 Hz, 1H), 4.05 (t, *J* = 6.1 Hz, 1H), 3.93 (t, *J* = 5.6 Hz, 1H), 3.79 (dd, *J* = 11.7, 2.1 Hz, 1H), 3.70–3.58 (m, 2H), 3.48 (dd, *J* = 9.1, 5.3 Hz, 1H), 3.31–3.22 (m, 2H), 1.17 (t, *J* = 7.2 Hz, 3H).

<sup>13</sup>C{<sup>1</sup>H} NMR (151 MHz, Methanol-*d*<sub>4</sub>) δ 163.1, 90.9, 76.3, 75.8, 75.7, 71.2, 63.3, 39.6, 14.9.

HR-ESI-MS calculated for C<sub>9</sub>H<sub>16</sub>N<sub>2</sub>O<sub>4</sub>S [M + H]<sup>+</sup> 249.0831, found 249.0904.

## ■ ASSOCIATED CONTENT

### Supporting Information

The Supporting Information is available free of charge at <https://pubs.acs.org/doi/10.1021/acsomega.4c06141>.

Table of synthetic conditions tested, <sup>1</sup>H and <sup>13</sup>C NMR spectra, and HPLC chromatogram of recrystallized Thiamet-G (PDF)

## ■ AUTHOR INFORMATION

### Corresponding Author

David J. Vocadlo – Department of Chemistry, Simon Fraser University, Burnaby, British Columbia V5S 1P6, Canada; Department of Molecular Biology and Biochemistry, Simon Fraser University, Burnaby, British Columbia V5S 1P6, Canada; [orcid.org/0000-0001-6897-5558](https://orcid.org/0000-0001-6897-5558); Email: [dvocadlo@sfu.ca](mailto:dvocadlo@sfu.ca)

### Authors

Viktor Holicek – Department of Chemistry, Simon Fraser University, Burnaby, British Columbia V5S 1P6, Canada; [orcid.org/0000-0002-1747-3600](https://orcid.org/0000-0002-1747-3600)

Matthew Deen – Department of Chemistry, Simon Fraser University, Burnaby, British Columbia V5S 1P6, Canada

Sandeep Bhosale – Department of Chemistry, Simon Fraser University, Burnaby, British Columbia V5S 1P6, Canada

Roger A. Ashmus – Department of Chemistry, Simon Fraser University, Burnaby, British Columbia V5S 1P6, Canada; [orcid.org/0000-0001-9580-7533](https://orcid.org/0000-0001-9580-7533)

Complete contact information is available at:

<https://pubs.acs.org/doi/10.1021/acsomega.4c06141>

### Notes

The authors declare the following competing financial interest(s): DJV is a cofounder of and holds equity in the company Alectos Therapeutics. DJV serves as CSO and Chair of the Scientific Advisory Board (SAB) of Alectos Therapeutics. DJV may receive royalties from SFU for commercialization of technology relating to OGA inhibitors.

## ■ ACKNOWLEDGMENTS

We are grateful for support from the Weston Foundation (PJT-156202) and the Natural Sciences and Engineering Council of Canada (NSERC, RGPIN-05426). D.J.V. thanks the Canada Research Chairs program for support as a Tier I Canada Research Chair in Chemical Biology. M.C.D. thanks NSERC for support through a PGS-D scholarship.

## ■ REFERENCES

- Whelan, S. A.; Hart, G. W. Proteomic Approaches to Analyze the Dynamic Relationships between Nucleocytoplasmic Protein Glycosylation and Phosphorylation. *Circ. Res.* **2003**, *93* (11), 1047–1058.
- Khidekel, N.; Ficarro, S. B.; Peters, E. C.; Hsieh-Wilson, L. C. Exploring the O-GlcNAc proteome: Direct identification of O-GlcNAc-modified from the brain. *Proc. Natl. Acad. Sci. U. S. A.* **2004**, *101* (36), 13132–13137.
- Ishimura, E.; Nakagawa, T.; Moriwaki, K.; Hirano, S.; Matsumori, Y.; Asahi, M. Augmented O-GlcNAcylation of AMP-activated kinase promotes the proliferation of LoVo cells, a colon cancer cell line. *Cancer Sci.* **2017**, *108* (12), 2373–2382.
- Olivier-Van Stichelen, S.; Dehennaut, V.; Buzy, A.; et al. O-GlcNAcylation stabilizes  $\beta$ -catenin through direct competition with phosphorylation at threonine 41. *FASEB J.* **2014**, *28* (8), 3325–3328.

- (5) Ding, N.; Ping, L.; Shi, Y.; et al. Thiamet-G-mediated inhibition of O-GlcNAcase sensitizes human leukemia cells to microtubule-stabilizing agent paclitaxel. *Biochem. Biophys. Res. Commun.* **2014**, *453* (3), 392–397.
- (6) Jaskiewicz, N. M.; Townson, D. H. Hyper-O-GlcNAcylation promotes epithelial-mesenchymal transition in endometrial cancer cells. *Oncotarget.* **2019**, *10* (30), 2899–2910.
- (7) Zhu, Y.; Shan, X.; Yuzwa, S. A.; Vocadlo, D. J. The emerging link between O-GlcNAc and Alzheimer disease. *J. Biol. Chem.* **2014**, *289* (50), 34472–34481.
- (8) Congdon, E. E.; Sigurdsson, E. M. Tau-targeting therapies for Alzheimer disease. *Nat. Rev. Neurol.* **2018**, *14* (7), 399–415.
- (9) Yuzwa, S. A.; Shan, X.; Jones, B. A.; et al. Pharmacological inhibition of O-GlcNAcase (OGA) prevents cognitive decline and amyloid plaque formation in bigenic tau/APP mutant mice. *Mol. Neurodegener.* **2014**, *9*, 42.
- (10) Pinho, T. S.; Correia, S. C.; Perry, G.; Ambrósio, A. F.; Moreira, P. I. Diminished O-GlcNAcylation in Alzheimer's disease is strongly correlated with mitochondrial anomalies. *Biochim Biophys Acta - Mol. Basis Dis.* **2019**, *1865* (8), 2048–2059.
- (11) Levine, P. M.; Galesic, A.; Balana, A. T.; et al.  $\alpha$ -Synuclein O-GlcNAcylation alters aggregation and toxicity, revealing certain residues as potential inhibitors of Parkinson's disease. *Proc. Natl. Acad. Sci. U. S. A.* **2019**, *116* (5), 1511–1519.
- (12) Gao, Y.; Wells, L.; Comer, F. I.; Parker, G. J.; Hart, G. W. Dynamic O-glycosylation of nuclear and cytosolic proteins: Cloning and characterization of a neutral, cytosolic  $\beta$ -N-acetylglucosaminidase from human brain. *J. Biol. Chem.* **2001**, *276* (13), 9838–9845.
- (13) Selnick, H. G.; Hess, J. F.; Tang, C.; et al. Discovery of MK-8719, a Potent O-GlcNAcase Inhibitor as a Potential Treatment for Tauopathies. *J. Med. Chem.* **2019**, *62* (22), 10062–10097.
- (14) Permanne, B.; Sand, A.; Ousson, S.; et al. O-GlcNAcase Inhibitor ASN90 is a Multimodal Drug Candidate for Tau and  $\alpha$ -Synuclein Proteinopathies. *ACS Chem. Neurosci.* **2022**, *13* (8), 1296–1314.
- (15) Shcherbinin, S.; Kielbasa, W.; Dubois, S.; et al. Brain target occupancy of LY3372689, an inhibitor of the O-GlcNAcase (OGA) enzyme: Translation from rat to human. *Alzheimers Dement.* **2020**; *16* (S4). doi:.
- (16) Yuzwa, S. A.; Macauley, M. S.; Heinonen, J. E.; et al. A potent mechanism-inspired O-GlcNAcase inhibitor that blocks phosphorylation of tau in vivo. *Nat. Chem. Biol.* **2008**, *4* (8), 483–490.
- (17) Cekic, N.; Heinonen, J. E.; Stubbs, K. A.; et al. Analysis of transition state mimicry by tight binding aminothiazoline inhibitors provides insight into catalysis by human: O-GlcNAcase. *Chem. Sci.* **2016**, *7* (6), 3742–3750.
- (18) Macauley, M. S.; He, Y.; Gloster, T. M.; Stubbs, K. A.; Davies, G. J.; Vocadlo, D. J. Inhibition of O-GlcNAcase Using a Potent and Cell-Permeable Inhibitor Does Not Induce Insulin Resistance in 3T3-L1 Adipocytes. *Chem. Biol.* **2010**, *17* (9), 937–948.
- (19) Kim, H. B.; Lee, S. W.; Mun, C. H.; et al. O-linked N-acetylglucosamine glycosylation of p65 aggravated the inflammation in both fibroblast-like synoviocytes stimulated by tumor necrosis factor- $\alpha$  and mice with collagen induced arthritis. *Arthritis Res. Ther.* **2015**, *17* (1), 1–8.
- (20) Miguez, J. S. G.; Dela Justina, V.; Bressan, A. F. M.; et al. O-Glycosylation with O-linked  $\beta$ -N-acetylglucosamine increases vascular contraction: Possible modulatory role on Interleukin-10 signaling pathway. *Life Sci.* **2018**, *209* (July), 78–84.
- (21) Soulié, M.; Beseme, O.; Nicol, L.; et al. O-GlcNAcase inhibition by Thiamet G opposes acute cardiac decompensation in rats with chronic heart failure. *Arch Cardiovasc Dis Suppl.* **2019**, *11* (2), 229.
- (22) Jiang, M.; Yu, S.; Yu, Z.; et al. XBP1 (X-Box-Binding Protein-1)-Dependent O-GlcNAcylation Is Neuroprotective in Ischemic Stroke in Young Mice and Its Impairment in Aged Mice Is Rescued by Thiamet-G. *Stroke.* **2017**, *48* (6), 1646–1654.
- (23) Zhu, Y.; Shan, X.; Safarpour, F.; et al. Pharmacological Inhibition of O-GlcNAcase Enhances Autophagy in Brain through an mTOR-Independent Pathway. *ACS Chem. Neurosci.* **2018**, *9* (6), 1366–1379.
- (24) Lee, B. E.; Kim, H. Y.; Kim, H. J.; et al. O-GlcNAcylation regulates dopamine neuron function, survival and degeneration in Parkinson disease. *Brain.* **2020**, *143* (12), 3699–3716.
- (25) Wang, X.; Smith, K.; Pearson, M.; et al. Early intervention of tau pathology prevents behavioral changes in the rTg4510 mouse model of tauopathy. Ginsberg SD, ed. *PLoS One* **2018**, *13* (4), No. e0195486.
- (26) Grima, J. C.; Daigle, J. G.; Arbez, N.; et al. Mutant Huntingtin Disrupts the Nuclear Pore Complex. *Neuron* **2017**, *94* (1), 93–107.e6.
- (27) Hastings, N. B.; Wang, X.; Song, L.; et al. Inhibition of O-GlcNAcase leads to elevation of O-GlcNAc tau and reduction of tauopathy and cerebrospinal fluid tau in rTg4510 mice. *Mol. Neurodegener.* **2017**, *12* (1), 1–16.
- (28) Andrés-Bergós, J.; Tardío, L.; Larranaga-Vera, A.; Gómez, R.; Herrero-Beaumont, G.; Largo, R. The increase in O-linked N-acetylglucosamine protein modification stimulates chondrogenic differentiation both in vitro and in vivo. *J. Biol. Chem.* **2012**, *287* (40), 33615–33628.
- (29) McGreal, S. R.; Bhushan, B.; Walesky, C.; et al. Modulation of O-GlcNAc levels in the liver impacts acetaminophen-induced liver injury by affecting protein adduct formation and glutathione synthesis. *Toxicol. Sci.* **2018**, *162* (2), 599–610.
- (30) Cunha, A. C.; Pereira, L. O. R.; De Souza, M. C. B. V.; Ferreira, V. F. Use of protecting groups in carbohydrate chemistry: An advanced organic synthesis experiment. *J. Chem. Educ.* **1999**, *76* (1), 79–80.
- (31) Heath, J. M.; Sun, Y.; Yuan, K.; et al. Activation of AKT by O-linked N-Acetylglucosamine induces vascular calcification in diabetes mellitus. *Circ. Res.* **2014**, *114* (7), 1094–1102.
- (32) Barrett, G. C.; Khokhar, A. R. Trifluoroacetic Acid as a Cyclisation Reagent for the Synthesis of Thiazol5(4H)-ones and 2-Thiazolines. *J. Chem. Soc. C* **1969**, *8*, 1117–1119.